Lithospheric dynamics and tectonic- stratigraphic evolution of the Ebro Basin

Zoetemeijer, R.; Desegaulx, P.; Cloetingh, S.A.P.L.; Roure, F.; Moretti, I.

published in
Journal of Geophysical Research
1990

DOI (link to publisher)
10.1029/JB095iB03p02701

document version
Publisher's PDF, also known as Version of record

JOURNAL OF GEOPHYSICAL RESEARCH, VOL. 95, NO. B3, PAGES 2701–2711, MARCH 10, 1990

Lithospheric Dynamics and Tectonic-Stratigraphic Evolution of the Ebro Basin

R. ZOETEMEIJER,[1] P. DESEGAULX,[2] S. CLOETINGH,[1] F. ROURE,[2] AND I. MORETTI[2]

We present analysis of two-dimensional modeling of the tectonic subsidence in the Ebro Basin along three profiles crossing the Pyrenees, the Ebro Basin, and the Catalan Coastal Range to the east, and the Iberic Cordillera to the west. The deformation of the foreland basin during Tertiary times is simulated using a lithospheric flexure model, incorporating laterally varying elastic thicknesses. The deflection of the plate is the combined result of Pyrenean loading and the loads exerted by the Iberic Cordillera and Catalan Coastal Range. In the eastern part of the Ebro Basin no extra driving force on the Iberian plate is required. The flexural modeling supports the hypothesis that underplating of the Iberian plate under the European plate is not associated with subduction of old oceanic lithosphere. A good fit with the Tertiary basin subsidence data and Bouguer anomalies is obtained for an elastic plate with local weakness zones under the Ebro Basin. The inferred lateral variation in the elastic rigidity is consistent with heat flow measurements in northern Spain and with major Mesozoic extension in the Iberic Cordillera and Valencia Trough.

INTRODUCTION

During the last 10 years much progress has been made in understanding the subsidence mechanisms of foreland basins [*Beaumont*, 1981; *Jordan*, 1981]. Modeling studies have revealed that subsidence in foreland basins is strongly influenced by the flexural response of the lithosphere to topographic loading. At the same time it has been demonstrated that the topographic load in itself is not always sufficient to explain the observed deflection of the foreland [*Lyon-Caen and Molnar*, 1983; *Angevine and Flanagan*, 1987; *Moretti and Royden*, 1988]. The hypothesis of simple convergent systems with emplacement of thrusts has recently made place for models of complex convergent zones with subduction zone structures. Simultaneously, analysis of lithospheric deflection has yielded adequate flexural models for these tectonically complex regions. In this paper we focus on the tectonic-stratigraphic evolution of the Ebro Basin that flanks the Pyrenees at the Spanish side. The Ebro foreland basin was formed in Paleogene to Aquitanian times in response to Pyrenean orogeny [*Puigdefabregas et al.*, 1986]. The foreland basin phase was preceded by Late Paleozoic-Early Mesozoic rifting, Early-Middle Cretaceous platform development and a phase of Middle Cretaceous (Albian) wrench tectonics [*Puigdefabregas and Souquet*, 1986]. The Late Paleozoic and Mesozoic structures are related to the opening of the Tethys, the Bay of Biscay, and the Atlantic Ocean and probably have strongly influenced the rheological properties of the Iberian plate underlying the Cenozoic Ebro Basin.

Wide-angle refraction measurements beneath the Pyrenees [*Daignieres et al.*, 1982] have demonstrated a drastic change in the depth of the Moho at the transition of the European and Iberian plate at the position of the North Pyrenean fault (NPF). Thickening of the Iberian crust was at that time attributed to continuous deformation in the crust nearby the left lateral North Pyrenean Fault [*Mattauer*, 1968, 1985; *Choukroune*, 1976]. Using this early model, *Brunet* [1986] proposed a flexural model of the Pyrenean belt with the existence of a crustal root due to the shortening induced by the convergence of Iberia towards Europe. Recently, a new ECORS deep seismic reflection profile crossing the entire Pyrenean orogenic belt has been completed [*Choukroune et al.*, 1990*b*]. The interpretation of the ECORS profile highlights the partial subduction of the Iberian continental lithosphere underneath the European continent, and effectively now images a drastic increase in crustal thickness [*Roure et al.*, 1989]. Simultaneously, subsidence analysis of the Ebro Basin by *Desegaulx and Moretti* [1988] have provided evidence for the potential importance of the Iberic Cordillera and Catalan Coastal Range on the present geometry of the basin.

In the present study we examine quantitatively the combined effect of the Pyrenees, the Iberic Cordillera, and the Catalan Coastal Range on the flexural evolution of the Ebro Basin. A flexural analysis of three profiles in the Ebro Basin suggests that the topographic load is sufficient to result in the observed gravity field and lithospheric deflection. A further new feature in the flexural model is the incorporation of laterally varying elastic rigidity. In particular, we demonstrate that local effects of preorogenic evolution and heat flow have

[1] Department of Earth Sciences, Vrije Universiteit, Amsterdam, The Netherlands

[2] Institut Francais du Petrole, Rueil Malmaison, France

Paper number 89JB03149.
0148-0227/90/89JB-03149$05.00

strongly influenced the rheological properties of the Iberian plate.

TECTONIC SETTING

The Ebro Basin is one of the largest (60,000 km^2) and deepest (about 4 km in the north) Tertiary basins of the Iberic Peninsula (Figure 1). To the north it is bounded by the E-W striking Pyrenean belt which forms the suture between the Iberian and the European plates. To the northeast, the Ebro basin is bounded by the NE-SW Catalan Coastal Range, while to the southwest the basin is bounded by the NW-SE Iberic Cordillera. The connection between these two chains is the structural complex "linking zone" [*Guimera*, 1984]. All these chains, (i.e., the Pyrenees, the Iberic Cordillera, and the Catalan Coastal Range) are emplaced on Cretaceous basins and result from the Paleogene N-S collision of Europe and Iberia [*Guimera*, 1984].

The Ebro Basin is located between the southward verging thrusts of the South Pyrenean Zone and Basque Massifs and the approximately northward verging Paleogene thrust units of the northern border of the Iberic Cordillera and Catalan Coastal Range (Figure 1). Seismic data also demonstrate that blind thrusting occurs north of the most external verging thrust in the western part of the Iberic Cordillera [*Anadon et al.*, 1985]. Paleogene compressive tectonics is often guided by preorogenic structures [*Alvaro and Guimera*, 1990]: dextral reactivation of late Hercynian NW-SE faults for the Iberic Cordillera and sinistral reactivation of the NE-SW faults for the Catalan Coastal Range [*Simon Gomez*, 1984] (see Figure 1). In the southern area of the linking zone the preorogenic structures are probably related to the Mesozoic extension. The main decollement level is generally situated in the Keuper [*Alvaro and Guimera*, 1990], but the Paleozoic basement is locally involved, and deeper levels of decollement occur probably in the Carboniferous and in the Silurian pelitic sequences [*Choukroune et al.*, 1990*a*]. During the early Miocene, the whole area (except the NW of the Iberic Cordillera) was subject to a NW-SE extension related to rifting events in the western Mediterranean [*Mauffret*, 1979], coeval with the opening of the Provencal Basin and the rotation of Corsica and Sardinia [*Burrus*, 1984].

The exploration wells used in the present study [*Instituto Geologico y Minero de Espana (IGME)*, 1987] show that the Tertiary basin deepens towards the Pyrenees. The main Tertiary sedimentary troughs are located close to the South Pyrenean Frontal Thrusts; 3580 m of Cenozoic beds have been drilled in well Sanguesa 1 and 2446 m in well Monzon 1 (Figure 1). In well Caspe 1, situated in the southernmost part of the Ebro Basin only 277 m of Cenozoic have been measured. The Paleogene strata that fill the Ebro Basin, were deposited in a variety of settings ranging from deep and shallow marine environments to nonmarine settings [*Puigdefabregas et al.*, 1986].

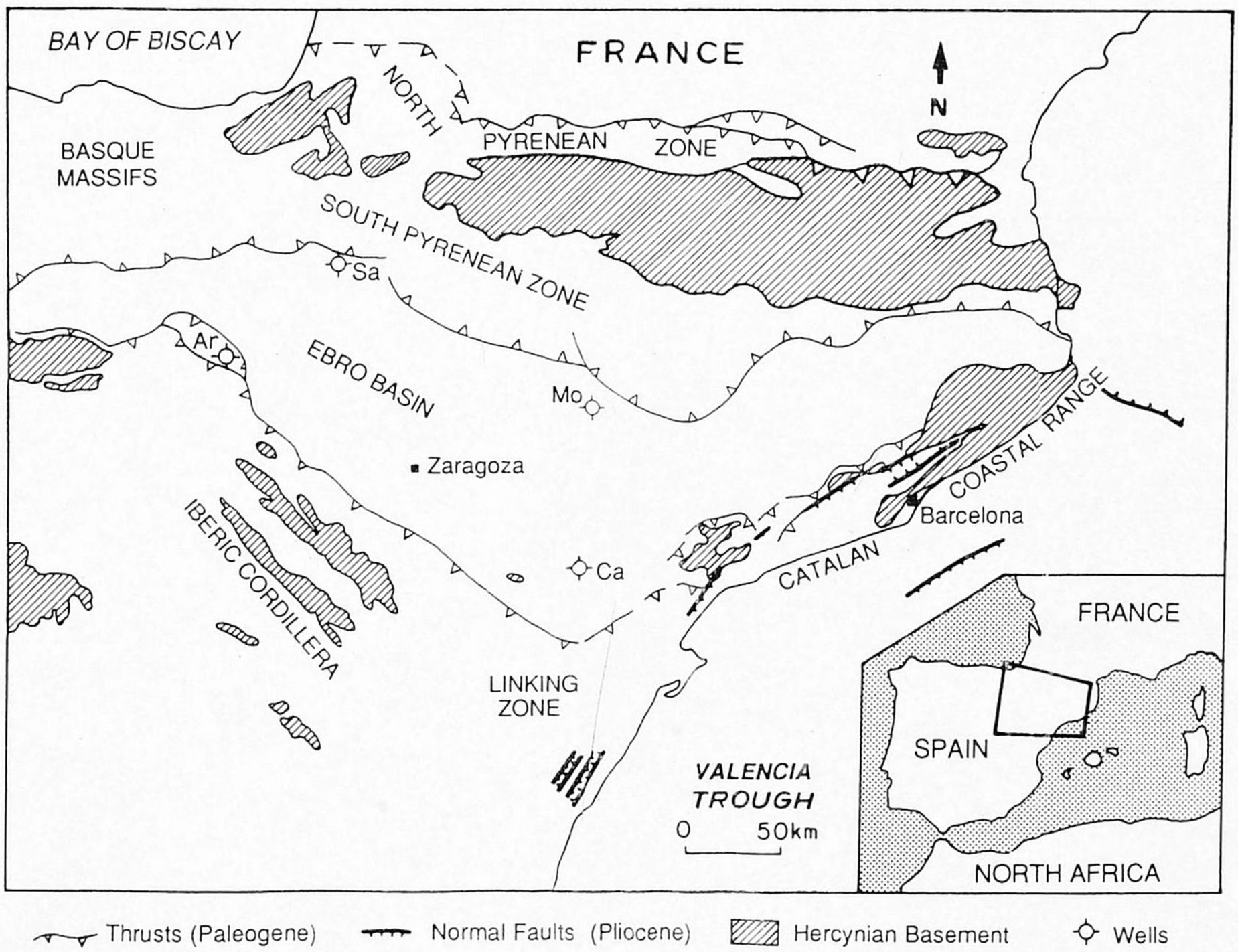

Fig. 1. Structural map of the Ebro Basin and surrounding mountain chains. The inset gives the location of the study area. Symbols used for the wells: Sa, Sanguesa 1; Mo, Monzon 1; Ar, Arnedo 1; Ca, Caspe 1 [after *IGME*, 1987].

GEOPHYSICAL DATA

The recent ECORS deep seismic profile across the Pyrenees [*ECORS Pyrenees Team*, 1988; *Choukroune et al.*, 1990*b*] (Figure 2) has imaged for the first time the entire crust of the chain. It provides new constraints necessary to restore the collision zone involving the European and Iberian plates palinspastically and has yielded an minimum estimate of 100 km shortening [*Roure et al.*, 1989]. The profile also shows the bending of the Iberian plate underneath the European plate and the asymmetric shape of the Tertiary Ebro Basin (Figure 2).

An important extension of previous modeling by *Desegaulx and Moretti* [1988] is the incorporation of Bouguer anomaly data in the present analysis. The Bouguer anomaly data used in this study are a compilation of maps from *Bureau de Recherches Geologiques et Minieres (BRGM)* [1974] and the Bouguer anomaly map of Catalonia [*Torne et al.*, 1988]. For the southernmost part of the Ebro Basin and SW of the Iberic Cordillera no data were available. Seismic refraction profiles [*Banda*, 1987] provide estimates for crustal thicknesses in the NE of Spain. In the southern part of the Ebro Basin the crustal thickness is about 30 km. In the central part of the Iberic Cordillera Moho depths can reach 32-35 km, especially near the linking zone (Figure 3). Toward the north, the Moho of the Iberian plate deepens progressively under the Pyrenees to reach a maximum depth of 50 km at the position of the surface trace of the NPF. The ECORS profile demonstrates that the excessive thickness of the crust of the Iberian plate results mainly from tectonic stacking of allochtonous nappes on a flexured autochtonous basement. Close to the Mediterranean shore line the Moho is recognized at a depth of 25 km. The shallowing of the Moho toward the Mediterranean is particularly pronounced in the area close to the Valencia Trough. As this thinning seems to affect partly the evolution of the Catalan Coastal Range, the linking zone and the Iberic Cordillera [*Banda*, 1987], it is doubtful that it is only related to Oligocene-early Miocene rifting events. An early thinning, Albian or older, can not be excluded. The heat flow map [*Cermak and Hurtig*, 1979] used in this study (Figure 4), shows high values south of the Ebro Basin (100 mW m^{-2}) and in the Valencia Trough (100 mW m^{-2}). Elsewhere values as low as (60 mW m^{-2}) are found. These observations are confirmed by recent heat flow measurements in the area [*Foucher et al.*, 1989].

MODELING OF LITHOSPHERIC FLEXURE AND GAVITY IN THE EBRO BASIN

The Iberian plate is modeled as an elastic plate, overlying an inviscid fluid (see the appendix). The plate is flexed down by a topographic load and a bordering trough, which is filled up by sediments. The numerical modeling technique allows us as a new feature to study the effects of lateral variations in the flexural rigidity. Simultaneously, we calculate the gravity anomaly that would result from the flexural model, using the method of *Parker* [1972] with Fourier transformations [*Bodine et al.*, 1981].

The two-dimensional modeling of lithospheric deflection is carried out for three approximately north-south located profiles, crossing the Pyrenees, the Ebro Basin, and the Iberic Cordillera to the west and the Catalan Coastal Range to the east (Figure 3). The data for the calculations are based on the exploration wells and Bouguer anomaly maps described in the previous section. Independent constraints are provided by deep seismic data and heat flow measurements. We ignore three-dimensional effects in the modeling. Numerical experiments demonstrate that this assumption [e.g., *Turcotte and Schubert*, 1982] is adequate for modeling of profiles 1 and 2. For the westernmost located profile 3, however, some effects of three dimensionality might affect the model predictions.

We first examine profile 1 with the hypothesis of a continuous plate. The gravity data are smooth and have a distinct wavelength. They suggest that the collision of the Iberian plate and the European plate created a situation in which the two plates are now continuous. The results of the deflection modeling (Figure 5*a*) show that a continuous elastic plate with an effective elastic thickness (EET) of 8 km gives a good fit to the wavelength of the

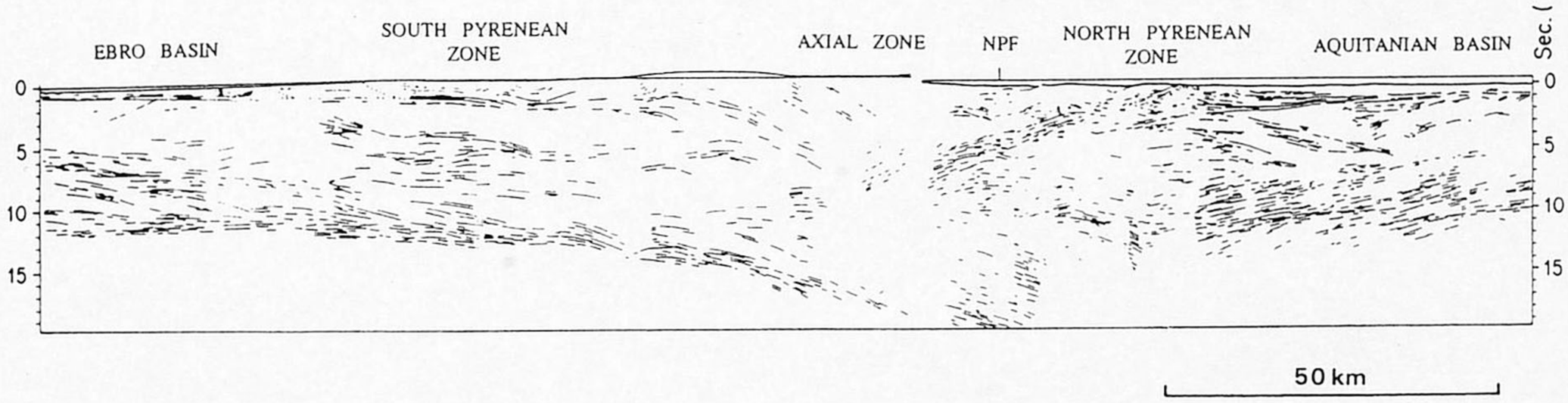

Fig. 2. Line drawing of the ECORS seismic deep reflection profile [after *ECORS Pyrenees Team*, 1988]. The location of the ECORS profile is given in Figure 3.

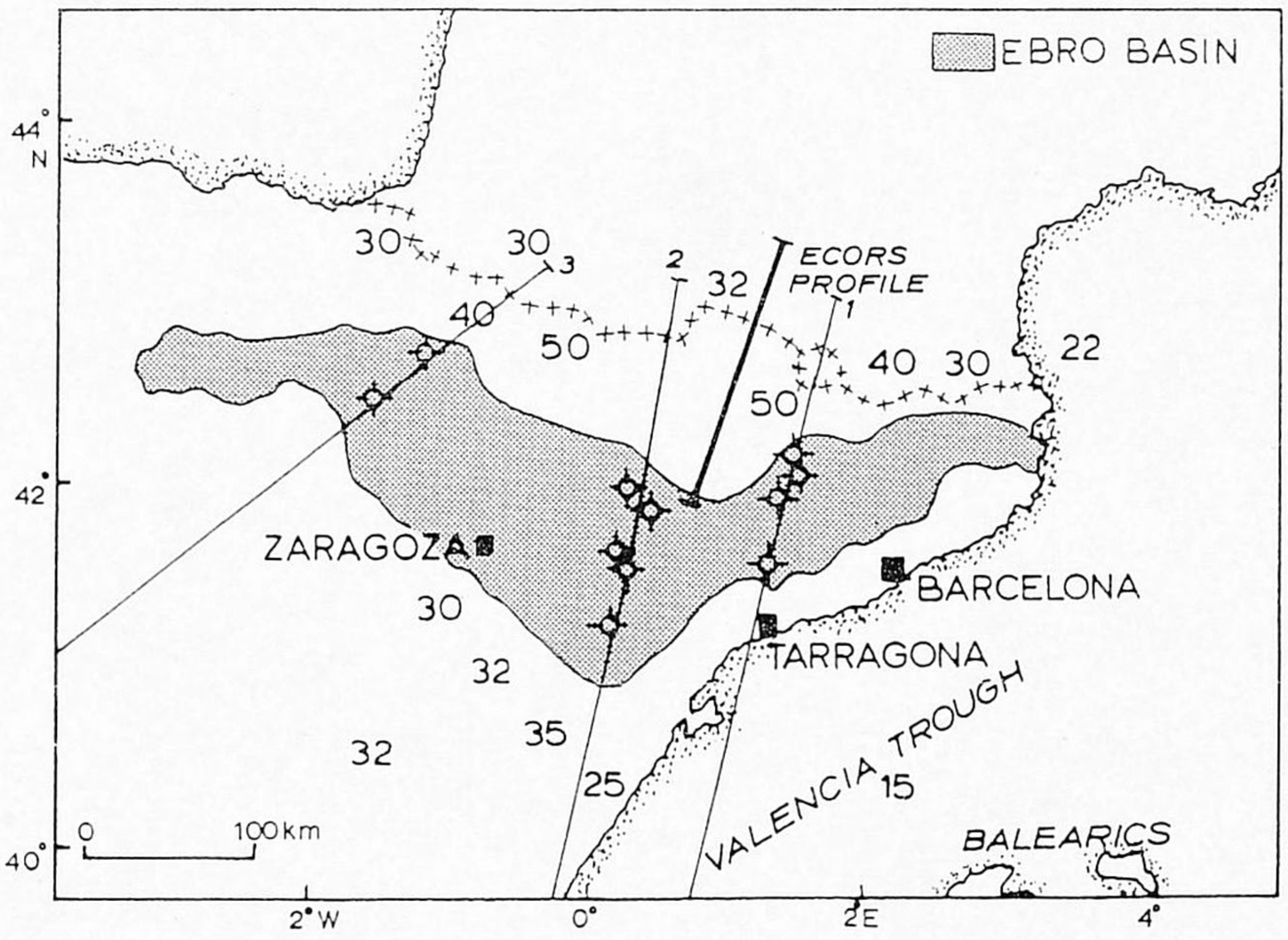

Fig. 3. Locations of the three profiles used in the flexural modeling (from the east to the west: Profiles 1, 2 and 3). The stars denote the position of the wells in the Ebro Basin. The heavy line gives the location of the ECORS profile. Also given are values of crustal thicknesses (in kilometers) inferred from refraction studies [after *Banda,* 1987].

Bouguer anomaly data; however, the profile is shifted laterally. The calculated Bouguer anomaly minimum lies 20 km to the north of the observed minimum. Moreover, for this value of the EET, the fit with the observed deflection is unsatisfactory. The very thin elastic plate compensates the topography almost isostaticaly. This leads to a deflection profile, which is symmetric to the topography, as shown in Figure 5*a*. For a stronger elastic plate with an EET of 20 km, this latter effect disappears, but the deflection is still not large enough to fit the data. Besides, the calculated shape of the anomaly profile is too wide. In order to solve these shortcomings a broken plate model is necessary, which is also better in agreement with the seismic data. Similarly, for the profiles 2 and 3 the pattern of the Bouguer anomaly data provides strong evidence for a broken plate situation.

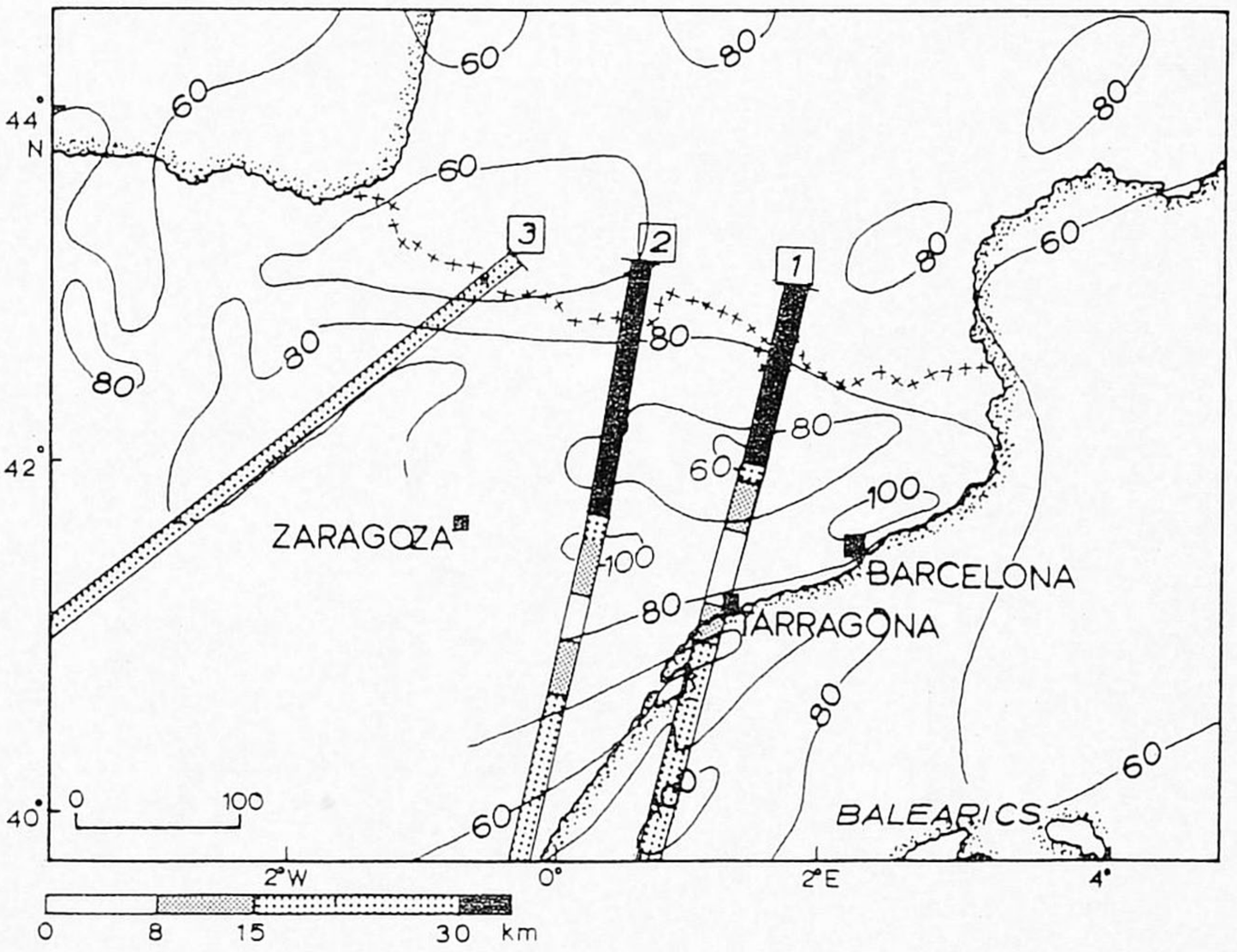

Fig. 4. Heat flow data of Northern Spain [after *Cermak and Hurtig,* 1979], with isolines in mW m^{-2}. Bars with different shading along the three profiles indicate the lateral variation in effective elastic thickness (EET) inferred from the flexural model.

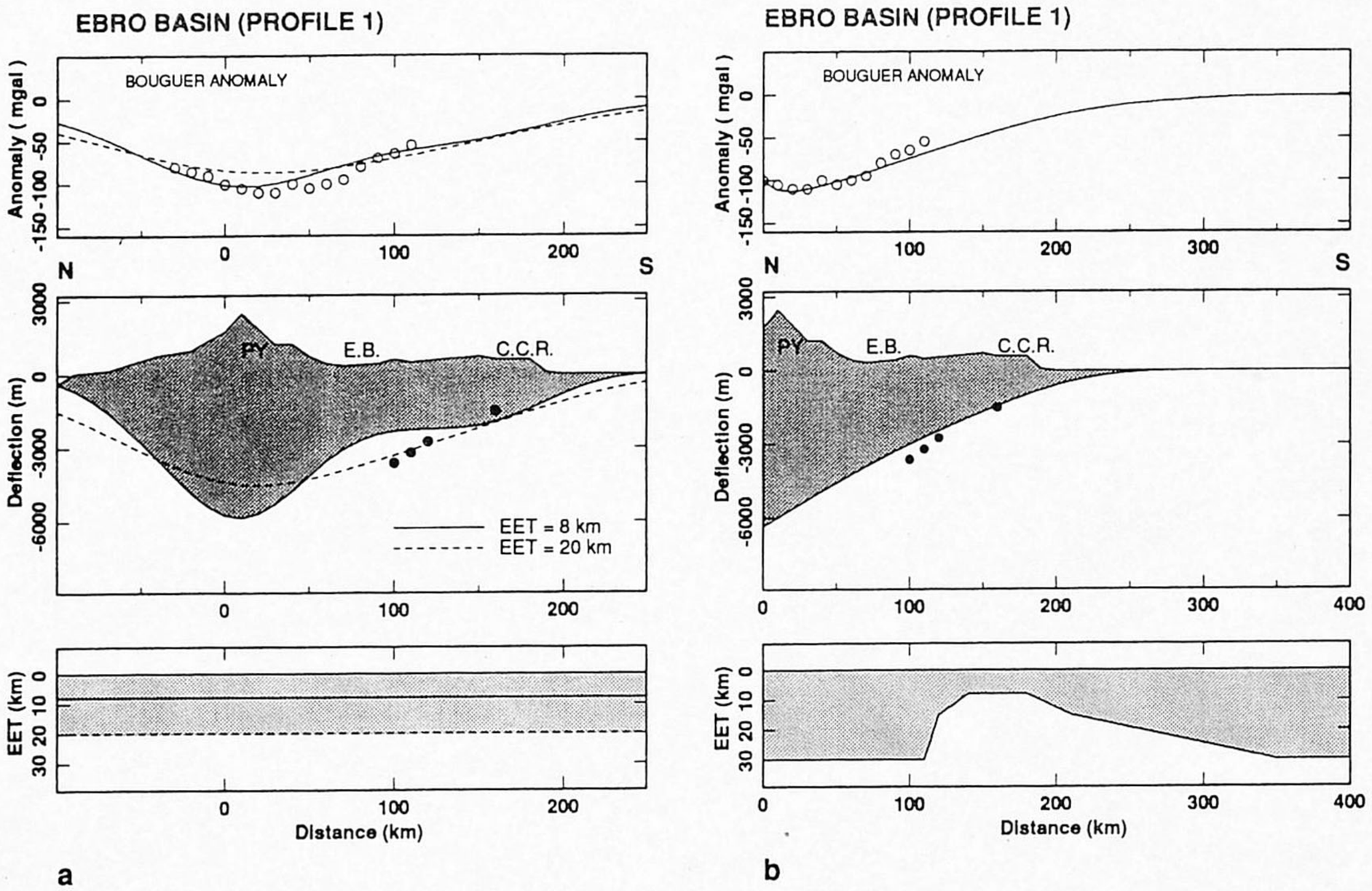

Fig. 5. Transect across the Pyrenees, Ebro Basin, and Catalan Coastal Range, (profile 1). *(a)* Results for a continuous plate. *(b)* Broken plate results. Open and solid circles indicate gravity anomaly data and depths of the Tertiary base, respectively. The solid and dashed lines show the calculated deflections and corresponding Bouguer anomaly of the Tertiary surface along profile 1. Dots indicate the position of the wells: Basella 1; Sanahuja 1; Guisona; Senant 1. $\rho_l = \rho_s = 2650$ kg/m^3, $\rho_c = 2750$ kg/m^3, $\rho_m = 3300$ kg/m^3, $P = 0.0$ N m^{-1}, $M = 0.0$ N. *(a)* The calculated deflections and Bouguer anomalies of two continuous plates with EET is 8 km and EET is 20 km. *(b)* The calculated deflection and Bouguer anomaly of the broken plate model with lateral variations of EET. Reduced values of EET occur between $x = 100$ km and $x = 350$ km.

In the broken plate model [e.g., *Royden*, 1988] the interaction between the Iberian and European plates can be taken into account by a vertical shear force P or bending moment M at the end of the plates. The broken plate boundary conditions (see the appendix) require the specification of these terminal parameters and assumptions for the position of the edge of the Iberian plate. As shown by recent geophysical data [*ECORS Pyrenees Team*, 1988], the maximum crustal thickness coincides with the location of the surface trace of the NPF. Similar to *Brunet* [1986], we adopt here the NPF trace as the northern boundary of the plunging Iberian plate. The results from the three profiles for the broken plate model will be discussed from east to west.

Profile 1

This profile is the easternmost transect and crosses the Pyrenees and Catalan Coastal Range. To the south the profile extends into the Mediterranean sea. The base of the Tertiary is constrained by four wells (Figure 5*b*) which clearly show deepening of the basin toward the Pyrenees. In order to fit the deflection at the position of the shallow well Senant 1, the plate has to bend strongly. A weakening of the elastic plate under the Catalan Coastal Range is therefore necessary. The weakening implies a decrease of elastic thickness from an EET of 30 km to an EET of 8 km. Our analysis is different from the earlier study of *Brunet* [1986] by taking into account the combined effect of Pyrenean loading and the loads exerted by the Iberic Cordillera and Catalan Coastal range. Also in contrast to *Brunet* [1986], the calculated results do not require any moment or load at the free end of the plate. The topographic load itself is sufficient to describe the basin geometry and gravity anomaly (Figure 5*b*).

Profile 2

The transect across the central part of the Ebro Basin, clearly shows the shallowness of the basin close to the Iberic Cordillera (Figure 6*a*). Because of the shallow basin depths (500 m) at approximately 100 km south of the South Pyrenean Frontal Thrust (SPFT) the deflection, due to the topographic loading of the Pyrenees, must be compensated largely to isostatic equilibrium. Similarly, the topographic load of the Iberic Cordillera must have been compensated, as it is even closer to the shallow part of the Ebro Basin than the Pyrenees in the north.

An elastic plate with an EET of 30 km would be sufficient to compensate the Pyrenean load along the Ebro Basin. The joint contribution of the Pyrenean load

and the Iberic Cordillera to the deflection of the lithosphere is shown in Figure 6*a*. For very low values of EET the basin shallows, while the asymmetric shape of the basin disappears for the value of 10 km for the EET A local weakening of the elastic plate between the Ebro Basin and the Iberic Cordillera is required in order to explain the existence of the Iberic topographic load (Figure 6*b*). This weak part of the lithosphere (EET=8 km) is situated at the southern part of the Ebro Basin. Similar to profile 1, the topographic load itself is sufficient to explain the observed basin geometry and gravity anomaly.

The measured Bouguer anomaly of profile 2 differs from the modeled anomaly with a constant value of about 25 mGal. Because of this constant trend in the misfit of the model results, the cause of this inadequacy is probably due to the choice of reference level. The Tertiary thickness of 277 m of the southernmost situated well Caspe 1 is not in agreement with the calculated deflection. A possible tectonic explanation for this misfit will be treated further on. Similarly, the implications of the inferred weakness zone will be discussed.

Profile 3

This profile is a transect through the narrow western part of the Ebro Basin. In contrast to the other two profiles it is NE-SW oriented (Figure 3). Due to the activity of the South Pyrenean Frontal Thrusts and thrusts of the Iberic Cordillera, the information of the Tertiary thickness in the narrow Ebro Basin is restricted to two wells (Figure 7).

In the north, the profile is close to the deep complex structure of the Aquitaine Basin at the NW side of the Pyrenees. The thick sedimentary wedge accumulated in the Aquitaine Basin is obviously an indication for the relative small negative or even positive Bouguer anomaly underneath the western Pyrenean zone. The adopted downwards pointing force ($P = 8.0 \times 10^{11}$ N m^{-1}, for an EET of 20 km) is probably associated with this feature. Future study of the subsidence history of the Aquitaine Basin [*Desegaulx et al.*, 1989] will likely yield important new constraints on the magnitude of this parameter.

The densities of load and infill, used in the model calculations, are both 2650 kg m^{-3}. This is an overestimation of the density for material near the surface but also an underestimation of the density for material at a great depth, under the Pyrenees. The effect of the overestimation becomes clear in the misfit of the Bouguer anomaly in the north of profile 1. A change of infill density from 2650 to 2750 kg m^{-3} at a depth of 4000 m and deeper, introduces an anomaly of about 30 mGal at the surface. However, the flexural effect of this density contrast has

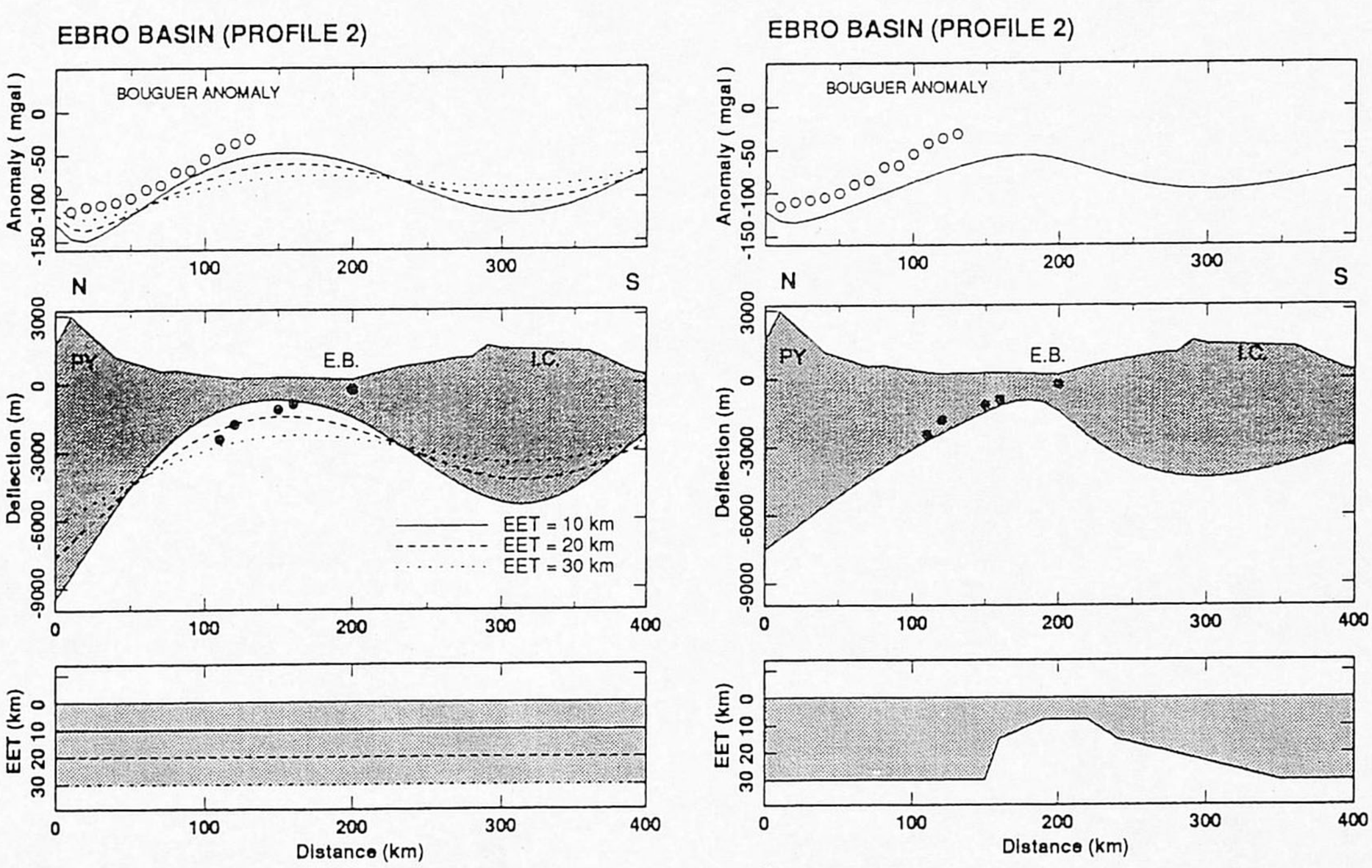

Fig. 6. Transect across the center of the Ebro Basin starting at the NPF, acoss the Pyrenees up to the Iberic Cordillera (profile 2). Open and solid circles indicate gravity anomaly data and depths of the Tertiary base, respectively. The solid and dashed lines show the calculated deflections and corresponding Bouguer anomaly of the Tertiary surface for different plate models. From north to south we used the following wells: Monzon 1; Esplus; Ballobar 1; Candasnos 1; Caspe 1. $\rho_i = \rho_s = 2650$ kg/m^3, $\rho_c = 2750$ kg/m^3, $\rho_m = 3300$ kg/m^3, $P = 0.0$ N m^{-1}, $M = 0.0$ N. *(a)* The calculated deflections and anomalies for the broken plate model with three different constant values of EET, 10, 20 and 30 km, respectively. *(b)* The calculated deflection and Bouguer anomaly of the broken plate model with lateral variations of EET. Reduced values of EET occur between $x = 140$ km and $x = 350$ km.

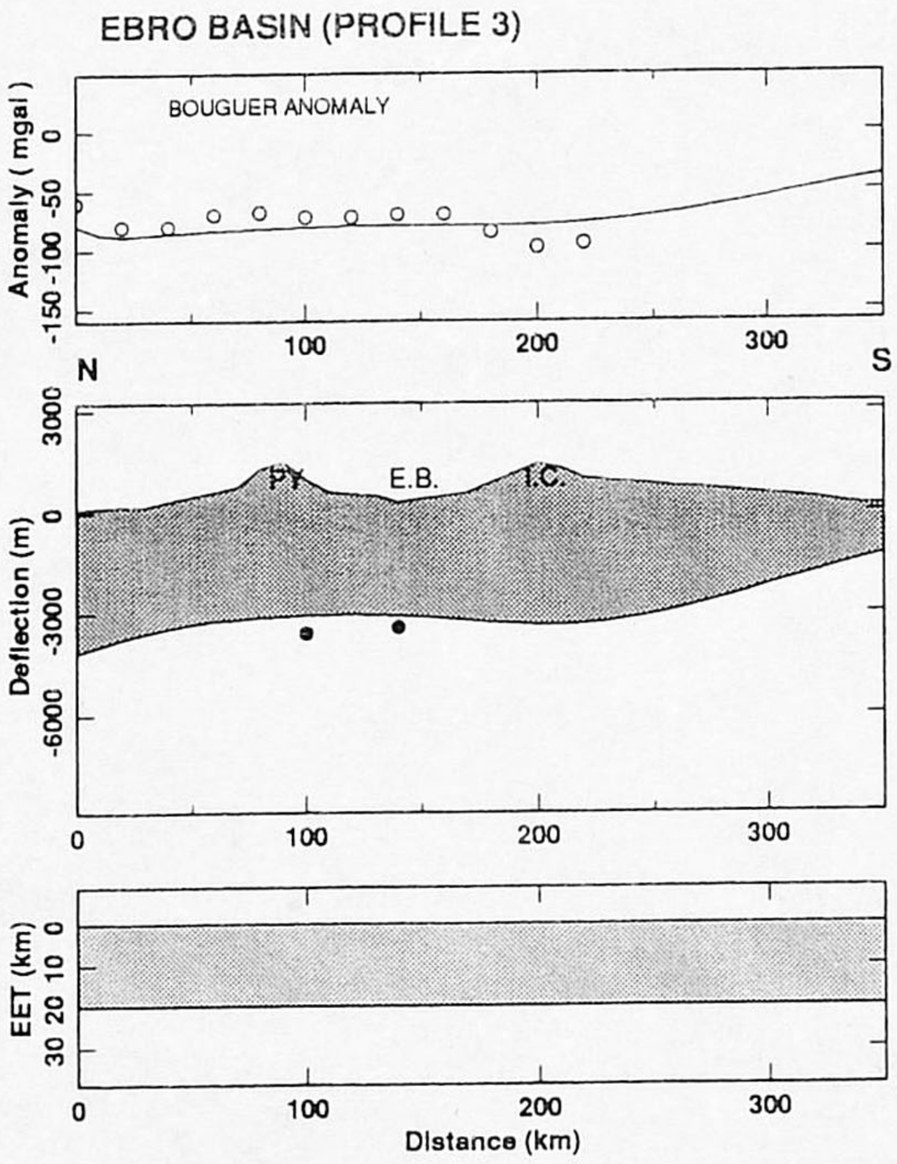

Fig. 7. The westernmost transect across the Pyrenees and Ebro Basin (profile 3). The topography south of the Ebro Basin is formed by the Iberic Cordillera and smoothly diminishes farther to the south, replacing the Meseta. The broken plate is modeled with an EET of 20 km. From north to south we used the following wells: Sanguesa 1; Marcilla 1. $\rho_l = \rho_s = 2650$ kg/m^3, $\rho_c = 2750$ kg/m^3, $\rho_m = 3300$ kg/m^3, $P = 8.0 \times 10^{11}$ N m^{-1}, $M = 0.0$ N.

also to be taken into account. This would imply a deepening of the basin and an extra infill with opposite anomaly contribution. Therefore the proposed positive Bouguer anomaly has to belong to a possibly preorogenic basin structure that is already flexurally compensated.

TECTONIC IMPLICATIONS FOR THE EVOLUTION OF THE IBERIAN PLATE

The mechanical consequences of the collision of the Iberic Peninsula and the European continent are expressed in the broken plate model, with lateral variations in elastic rigidity. These findings shed new light on the convergence of Iberia to Europe, the flexural interaction of the mountain chains, and the rheological variations of the lithosphere in the northern part of the Iberian plate.

Convergence of Iberia to Europe

The convergence of Iberia with respect to Europe is at least 100 km [*Seguret and Daignieres*, 1985; *Roure et al.*, 1989]. This value is more or less similar to the shortening of the sedimentary cover in the Apennine thrust belt, which was found to be around 150 km in the northern part and 80 km in the southern part of the Apennines [*Bally et al.*, 1986; *Endignoux et al.*, 1989]. The dynamics of the subduction process in the Iberian collision zone and the Apennines are, however, quite different. The sedimentary and thrust loads in the Apennines are too small to explain the subsidence of the foreland [*Royden and Karner*, 1984; *Moretti and Royden*, 1988], requiring an extra load representing a density pertubation associated with fossil subducted oceanic lithosphere. In the southern Apennines, subduction of old oceanic lithosphere occurs [*Gasparini et al.*, 1985; *Moretti and Royden*, 1988], and the present-day tectonic evolution images the transition between oceanic and continental subduction (P. Casero et al., Neogene geodynamic evolution of the southern Apennines, submitted to *Tectonics*, 1990). In contrast, the present study of the Ebro Basin strongly corroborates that the underplating of the Iberic Peninsula under the European plate is not associated with subduction of oceanic lithosphere. In particular, the model results of profiles 1 and 2 demonstrate that the topographic load itself is sufficient to describe the basin geometry, requiring no additional driving force on the plate. The modeling of profile 3, however, does not rule out the possibility of minor oceanic lithosphere subduction in the western part of the Ebro Basin.

Flexural Interaction of Mountain Chains and Reactivation of Preorogenic Structures

The overall shape of the Ebro Basin is clearly dominated by the Tertiary orogeny of its surrounding chains. This is particularly the case in the western part of the Ebro Basin, where the basin is narrowed by the Pyrenees and the Iberic Cordillera. The flexural interaction between these mountain chains results in a pronounced deflection in this area (profile 3), creating an approximately symmetric shape of the basin. In contrast, the asymmetric character of the deflection in profiles 1 and 2 reflects a reduced flexural interaction of the surrounding mountain chains in the eastern and central part of the Ebro Basin. The larger distance between the two chains and the weakness zones inferred from the modeling have reduced the effects of flexural interaction in this part of the Iberian plate.

The location of the Iberic Cordillera and Catalan Coastal Range, parallel to the Late Hercynean faults (Figure 1), indicates the importance of preexisting structures on the formation of the two chains. Although these structures are now essentially reactivated as strike-slip faults, important thrusting toward the Ebro Basin has also been found. The thrusting is important for the formation of topographic loads, as shown in the western part of the Ebro Basin. In this area blind thrusting has been recognized in seismic profiles [*Anadon et al.*, 1985]. The well Arnedo 1 (Figure 1) is situated on a thrust and shows an important decrease of thickness in the Tertiary strata in comparison with the depths measured in the basin (from 3580 to 850 m). In the south of the Ebro Basin a more or less similar situation occurs. The southernmost well used for profile 2 (Caspe 1) has also a very shallow Tertiary depth (277 m). Moreover, the structural map (Figure 1) shows a basement outcrop WSW of the well. The Paleozoic beds are exposed in a kilometric scale fold

which dips change from quite steep, northward dipping in the northern part, to southward dipping in the southern part of the outcrop. The statigraphy shows a syntectonic deposition of Tertiary beds on Paleozoic basement. Although seismic profiles were not available to support this idea, we interpret the shallowness of this well as a result of inversion tectonics, with Paleogene reactivation of a Late Hercynean normal fault in the foreland (Figure 8).

Lateral Variation in Rheological Properties of the Lithosphere Under the Ebro Basin

The increase of the crustal thickness under the Iberic Cordillera [*Banda*, 1987] is in agreement with the deflection modeled to compensate the Iberic Cordillera topography. In case, like under the Pyrenees, a completely broken lithosphere (EET=0 km) would be present under the Iberian Cordillera, the deflection would greatly exceed the deflection for local weakening with an EET of 8 km. Furthermore, the deflection of a broken plate is not consistent with the Moho depths measured from refraction data [*Banda*, 1987].

Also important is the similarity of the positions of the weakness zones and the places of elevated heat flow. The decrease in elastic thickness inferred by the flexural modeling reflects the weakening effect of elevated temperatures on the mechanical properties of the lithosphere. Although convenient, the characterization of lateral variations in mechanical behavior of the lithosphere in terms of an elastic plate provides only an indirect measure of the effect of temperature on lithospheric strength. A more accurate description of the actual strength distribution of the lithosphere, showing explicitly the dependence of strength on temperature, follows from laboratory experiments on the rheological properties of crustal and upper mantle rocks [*Goetze and Evans*, 1979]. To explore this dependence, we have constructed yield strength profiles of the continental lithosphere under the Ebro Basin based on extrapolation of rock mechanics data [*Brace and Kohlstedt*, 1980]. We have adopted an upper crust composed of quartz, a lower crust of diabase and an olivine composition for the upper mantle [*Caristan*, 1982; *Smith and Bruhn*, 1984]. Yield envelopes showing the temperature dependence of strength, for a continental lithosphere with 32-km-thick crust, are given in Figure 9. The spatial variation of the effective elastic thicknesses obtained from the flexural modeling of the Ebro Basin is in good agreement with the predictions of temperature-dependent strength of the lithosphere from laboratory data. Low values of EET correspond to reduced values of lithospheric strength. For example, an EET of 8 km, at the position of the local weakness zones inferred from the flexural model, is comparable with the cumulative strength of the yield envelope calculated for a heat flow of 100 mW m^{-2}. For a heat flow of 100 mW m^{-2}, the contribution of the upper crust dominates the strength of the lithosphere (Figure 9). For lower heat flow values, the contributions of the lower crust and upper mantle become more important yielding an increase in the lithospheric strength, equivalent to larger values of EET. As shown in Figure 9, an EET of 30 km is consistent with a lithospheric strength profile corresponding to a heat flow between 60 and 80 mW m^{-2}.

The reduced rigidity of the lithosphere provides strong support for the interpretation of the Iberic Cordillera as an aulacogen [*Alvaro et al.*, 1979]. This hypothesis indicates that the region of the intracontinental chain had recorded the premise of rifting. It is commonly thought that regions of continental extension are associated with local high geotherms and that strain in a continent is usually absorbed by its weak young parts. This suggests that especially the preorogenic Iberic Basin underwent strong deformation due to its weakened lithosphere at the time of collision of the Iberian Peninsula and the European continent. Furthermore, deposits on the Balearic Islands and on the Iberian Peninsula show very different sedimentary facies during Neocomian: continental sands to marine carbonates, shaly platform deposits on the Iberian Peninsula, and deep marine marly deposits on the Balearic Islands [*IGME*, 1987]. Similarly, nearby the linking zone as well, the Catalan thrust units show a west to east thickening of the Cretaceous sequences, with a transition from near shore to pelagic facies [*Guimera*, 1984]. These features strongly indicate that the extension in the Valencia Trough is of Neocomian age [*Roca and Desegaulx*, 1990], or a lateral continuation of the Aptian-Early Albian extension phase in the Iberic Cordillera [*Canerot*, 1985].

CONCLUSION

The polystaged evolution of the northern part of the Iberian Peninsula is responsible for the complex foreland basin development of the Ebro Basin. The present paper has demonstrated that the deflection of the Iberian plate under the Ebro Basin is due to the combined effect of loading exerted by the Pyrenees, the Iberic Cordillera, and the Catalan Coastal Range. The interaction between the different chains surrounding the Ebro Basin is pro-

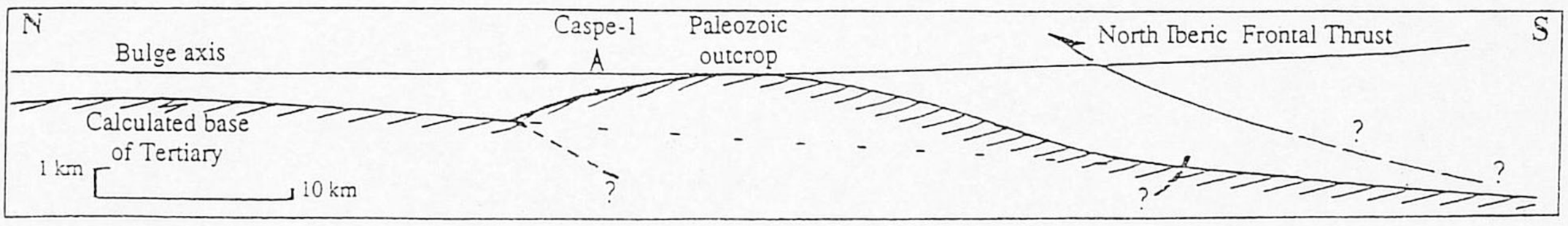

Fig. 8. Simplified sketch of the geological interpretation for the basement outcrop in the southern part of the Ebro Basin and explanation for the shallowness (277 m) of the well Caspe 1.

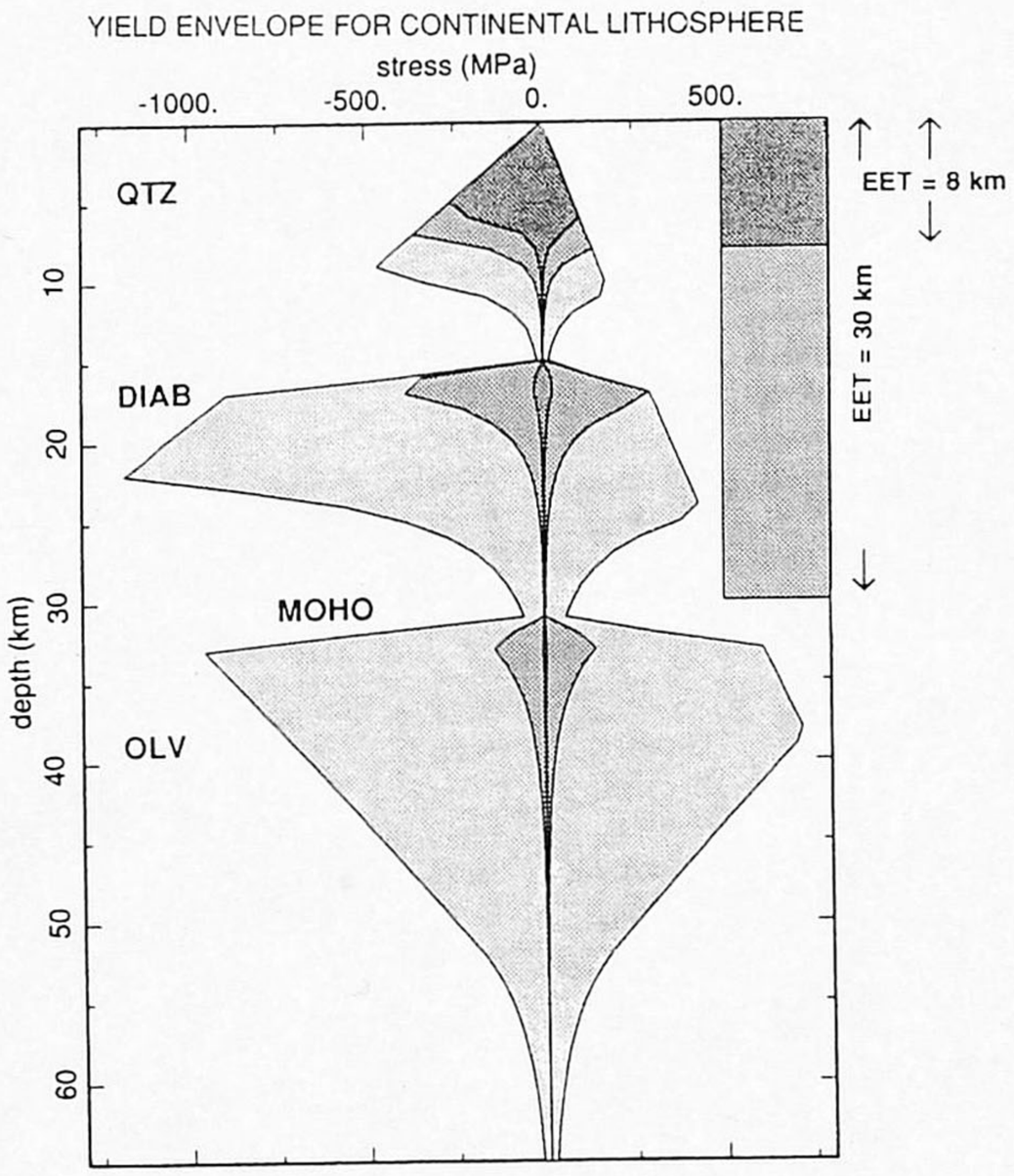

Fig. 9. Three yield envelopes for continental lithosphere with a 32 km thick crust with quartz/diabase/olivine composition [*Smith and Bruhn,* 1984; *Caristan,* 1982]. The darkest shading gives the envelope for a surface heat flow q_s of 100 mW m^{-2}, while progressively lighter shading shows the envelopes for q_s of 80, and 60 mW m^{-2}, respectively. The strain rate $\dot{\varepsilon}$ adopted in the extrapolation of the rock mechanics data is 10^{-16} s^{-1}. EET values of 30 and 8 km, inferred from the flexural model of the Ebro Basin are roughly consistent with lithospheric strength distributions calculated for a surface heat flow of about 70 and 100 mW m^{-2}, respectively.

nounced in the western part of the Ebro Basin where the basin has its main infill of Cenozoic beds. Parts of the Ebro Basin, where the well data indicate shallow Tertiary infill can be explained by Paleogene reactivation of preexisting faults. A new flexural analysis of three profiles in the Ebro Basin shows that the topographic loads themselves, due to thrusting, are able to explain the geometry of the Ebro Basin. No traction exerted by a subducted oceanic slab is required. The flexural modeling, therefore confirms that the Iberian collision was intracontinental. It thus differs from, for example, the Apennine collision zone, which followed an episode of oceanic subduction. An important tool used in the paper that goes beyond previous efforts is the incorporation of varying elastic thickness in the modeling. The local weakness zones predicted by the flexural modeling shed light on the heat flow anomalies in northern Spain. There is a correlation between observed heat flow and the elastic thicknesses inferred from the modeling of the foreland basin deflection. The results of our study strongly support an aulacogenic origin for the Iberic Cordillera. The recently put forward interpretation of a Mesozoic age for the extension phase in the Valencia Trough, is consistent with this tectonic scenario.

APPENDIX

The differential equation governing the deflection $w(x)$ of a thin elastic plate with variable rigidity $D(x)$, horizontal load N, and surface load $q(x)$ on top of a fluid mantle is

$$\frac{d^2}{dx^2}\left(D(x)\frac{d^2w}{dx^2}\right)+N\frac{d^2w}{dx^2}+(\rho_m-\rho_s)\,g\,w(x)=q(x) \quad (1)$$

with $g = 9.8$ m s^{-2} the gravity acceleration and $(\rho_m-\rho_s)$ is the density contrast of mantle and sedimentary infill.

The relationship between the flexural rigidity $D(x)$ and the thickness of the elastic plate $EET(x)$ is

$$D(x)=\frac{E\,(EET(x)^3)}{12(1-\nu^2)} \quad (2)$$

in which E is Young's modulus and ν is Poisson's ratio. In this study we adopt the following values: $E = 7.0\times10^{10}$ N m^{-2} and $\nu = 0.25$.

To solve the fourth-order differential equation (1) for bending, the elastic plate a finite difference approximation is used.

Boundary Conditions

As $x\to\infty$, $w(x)\to0$ and $dw/dx\to0$. The third and fourth boundary conditions for the broken plate are, at $x = 0$,

$$-D\left(\frac{d^2w}{dx^2}\right)\Bigg|_{x=0}=M_0 \quad (3)$$

with M_0 the bending moment applied at the free end of the plate (positive for counterclockwise).

$$\frac{d}{dx}D\left(\frac{d^2w}{dw^2}\right)\Bigg|_{x=0}=P_0 \quad (4)$$

where P_0 is the vertical shearforce applied at the free end of plate (down is positive).

Acknowledgements. We thank Joan Guimera and Maria Jose Jurado for constructive discussions in the field. Eduard Roca, Wim Groenewoud, Enric Banda, J.M. Fonbote, P. Santanach, Jilles van den Beukel, and Menno de Ruig are thanked for helpful suggestions. Charles Angevine and Peter Flemings provided thoughtful reviews. The Earth Science Institutes of Amsterdam and Utrecht and the Institut Francais du Petrole provided facilities that made the cooperative work possible. R.Z. and S.C. acknowledge partial support by NATO grant 0148/87.

REFERENCES

Alvaro, M., and J. Guimera, Structure et evolution de la compression alpine dans la chaine Iberique et la chaine Cotiere Catalane, *Bull. Soc. Geol. Fr.*, in press, 1990.

Alvaro, M., R. Capote, and R. Vegas, Un modelo de evolucion geotectonica para la Cadena Celtiberica, *Acta Geol. Hisp., 14*, 172–177, 1979.

Anadon, P., L. Cabrera, J. Guimera, and P. Santanach, Paleogene strike-slip deformation and sedimentation along the southeastern margin of the Ebro Basin, Strike-Slip Deformation, Basin Formation, and Sedimentation, edited by K.T. Biddle and N. Chistie-Blick, *Spec. Publ. Soc. Econ. Paleont. Mineral., 37*, 303–318, 1985.

Angevine, C.L., and K.M. Flanagan, Buoyant sub-surface loading of the lithosphere in the Great Plains Foreland Basin, *Nature, 327*, 137–139, 1987.

Bally, A., L. Burbi, C. Cooper, and R. Ghelardoni, Balanced sections and seismic reflection profiles across the Central Apennines, *Mem. Soc. Geol. It., 35*, 257–310, 1986.

Banda, E., Crustal parameters in the Iberian Peninsula, *Phys. Earth Planet. Inter., 51*, 222–225, 1987.

Beaumont, C., Foreland basins, *Geophys. J. R. Astron. Soc., 65*, 291–329, 1981.

Bodine, J.H., M.S. Steckler, and A.B. Watts, Observations of flexure and the rheology of the oceanic lithosphere, *J. Geophys. Res., 86*, 3695–3707, 1981.

Brace, W.F., and D.L. Kohlstedt, Limits on lithospheric stress imposed by laboratory experiments, *J. Geophys. Res., 85*, 6248–6252, 1980.

Bureau de Recherches Geologiques et Minieres, Elf-Re, Esso-Rep, SNPA, Geologie du basin d' Aquitaine, Orleans, 27 pp., 1974.

Brunet, M.F., The influence of the evolution of the Pyrenees on adjacent basins, *Tectonophysics, 129*, 343–354, 1986.

Burrus, J., Contribution to a geodynamic synthesis of the Provencal Basin (North-Western Mediterranean), *Mar. Geol., 55*, 247–269, 1984.

Canerot, J., La chaine Alpine de Iberides (Espagne); un example d' evolution sedimentaire et tectonique intraplaque, *Arch. Sci., 38*, 37–62, 1985.

Caristan, Y., The transition from high temperature creep to fracture in Maryland diabase, *J. Geophys. Res., 87*, 6781–6790, 1982.

Cermak, V., and E. Hurtig, Heat flow map of Europe, scale 1: 5,000,000 IUGG/IASPEI/IHFC, in Terrestrial Heat Flow in Europe, edited by V. Cermak and L. Rybach, 328 pp., Springer-Verlag, NewYork, 1979.

Choukroune, P., Structure et evolution tectonique de la zone North-Pyreneenne, analyse de la deformation dans une partie de chaine a schistosite sub-verticale, *Mem. Soc. Geol. Fr., 127*, 116 pp., 1976.

Choukroune, P., B. Pinet, F. Roure, and M. Cazes, Major Hercynian structures along the ECORS Pyrenees and Biscaye lines. *Bull. Soc. Geol. Fr.*, in press, 1990a.

Choukroune, P., F. Roure, B. Pinet, and ECORS Team, Main results of the ECORS Pyrenees profile, *Tectonophysics, 172*, in press, 1990b.

Daignieres, M., J. Gallart, E. Banda, and A. Hirn, Implications of the seismic structure for the orogenic evolution of the Pyrenean Range, *Earth Planet. Sci. Lett., 57*, 88–100, 1982.

Desegaulx, P., and I. Moretti, Subsidence history of the Ebro Basin, *J. Geodyn., 10*, 9–24, 1988.

Desegaulx, P., H. Kooi, S. Cloetingh, and I. Moretti, A subsidence model of the Aquitaine Basin during Cretaceous extension: Consequences on the plate behavior during the compression, paper presented at Meeting, Eur. Geophys. Soc., Barcelona, 1989.

ECORS Pyrenees Team, The ECORS deep reflection seismic survey across the Pyrenees, *Nature, 331*, 508–511, 1988.

Endignoux, L., I. Moretti, and F. Roure, Foreward modeling of the southern Apennines. *Tectonics, 8*, 1095–1104, 1989.

Foucher, J.P., A. Mauffret, B. Alonso, F. Harmegnies, J. Murillas, G. Ouillon, J.P. Rehault, M. Steckler, and E. Tzotzolakis, Heat flow results of the Valsis 1 cruise in the Gulf of Valencia, Western Mediteranean, *Terra Abstr., 1* (1), 48, 1989.

Gasparini, C., G. Iannaccone, P. Scandone, and R. Scarpa, Seismotectonics of the Calabrian Arc, *Tectonophysics, 84*, 267–286, 1985.

Goetze, C., and B. Evans, Stress and temperature in the bending lithosphere as constrained by experimental rock mechanics, *Geophys. J. R. Astron. Soc., 59*, 463–478, 1979.

Guimera, J., Paleogene evolution of the deformation in the northeastern Iberean Peninsula, *Geol. Mag., 121*, 413–420, 1984.

Instituto Geologico y Minero de Espana, *Contribucion de la Exploracion Petrolifera al Conocimiento de la Geologia de Espana*, 465 pp., Madrid, 1987.

Jordan, T.E., Thrust loads and foreland basin evolution, Cretaceous, western United States, *Am. Assoc. Pet. Geol. Bull., 65*, 2506–2520, 1981.

Lyon-Caen, H., and P. Molnar, Constraints on the structure of the Himalaya from an analysis of gravity anomalies and a flexural model of the lithosphere, *J. Geophys. Res., 88*, 8171–8191, 1983.

Mattauer, M., Les traits structuraux essentiels de la chaine Pyreneenne. *Rev. Geogr. Phys. Geol. Dyn., 10* (1), 3–11, 1968.

Mattauer, M., Presentation d' un modele lithospherique de la chaine des Pyrenees, *C. R. Acad. Sci., 300*, 71–74, 1985.

Mauffret, A., Etude geodynamique de la marge des iles Babeares, *Mem. Soc. Geol. Fr., 132*, 1–96, 1979.

Moretti, I., and L. Royden, Deflection, gravity and tectonics of doubly subducted continental lithosphere: Adriatic and Ionian Seas, *Tectonics, 7*, 875–893, 1988.

Parker, R.L., The rapid calculation of potential anomalies, *Geophys. J. R. Astron. Soc., 31*, 447–455, 1972.

Puigdefabregas, C., and P. Souquet, Tecto-sedimentary cycles and depositional sequences of the Mesozoic and Tertiary from the Pyrenees, *Tectonophysics, 129*, 173–203, 1986.

Puigdefabregas, C., J.A. Munoz, and M. Marzo, Thrust belt development in the eastern Pyrenees and related

depositional sequences in the southern foreland basin, *Spec. Publ. Int. Assoc. Sedimentol.*, *8*, 229–246, 1986.

Roca, E., and P. Desegaulx, Geodynamic evolution of the Valencia Trough from a Mesozoic extensional basin to the Early Miocene foredeep of the Betic-Balearic Chain, *Mar. Petr. Geol.*, in press, 1990.

Roure, F., P. Choukroune, and ECORS Pyrenees Team, ECORS deep seismic data and balanced cross sections: Geometric constraints on the evolution of the Pyrenees, *Tectonics*, *8*, 41–50, 1989.

Royden, L., Flexural behavior of the continental lithosphere in Italy: Constraints imposed by gravity and deflection data, *J. Geophys. Res.*, *93*, 7747–7766, 1988.

Royden, L., and G.D. Karner, Flexure of the lithosphere beneath the Apennine and Carpathian foredeep basins, *Nature*, *309*, 142–144, 1984.

Seguret, M., and M. Daignieres, Coupes balancees d' echelle crustale des Pyrenees, *C. R. Acad. Sci.*, *301*, 341–346, 1985.

Simon Gomez, J.L., Compression y distenssion alpinas en la Cadena Iberica oriental. Ph.D. thesis, 269 pp., Inst. Est. Eurolense, Zaragoza, Spain, 1984.

Smith, R.B., and R.L. Bruhn, Intraplate extensional tectonics on the eastern Basin-Range: Inferences of structural style from seismic reflection data, regional tectonics, and thermal-mechanical models of brittle- ductile deformation, *J. Geophys. Res.*, *89*, 5733–5762, 1984.

Torne, M., A. Cases, and E. Banda, Cartografia geofisica en Cataluna, II, El mapa gravimetrico, *Rev. Soc. Geol. Espana*, *1* 81–87, 1988.

Turcotte, D.L., and G. Schubert, *Geodynamics*, John Wiley, New York, 450 pp., 1982.

S. Cloetingh and R. Zoetemeijer, Department of Earth Sciences, Vrije Universiteit, P.O. Box 7161, 1007 MC Amsterdam, The Netherlands.

P. Desegaulx, I. Moretti, and F. Roure, Institut Francais du Petrole, 92506 Rueil Malmaison, France.

(Received March 15, 1989;
revised October 5, 1989;
accepted October 6, 1989.)